

## Experimental determination of a nonclassical Glauber-Sudarshan $P$ function

T. Kiesel and W. Vogel

*Arbeitsgruppe Quantenoptik, Institut für Physik, Universität Rostock, D-18051 Rostock, Germany*

V. Parigi

*Department of Physics, University of Florence, I-50019 Sesto Fiorentino, Florence, Italy*

*and LENS, Via Nello Carrara 1, 50019 Sesto Fiorentino, Florence, Italy*

A. Zavatta and M. Bellini

*LENS, Via Nello Carrara 1, 50019 Sesto Fiorentino, Florence, Italy*

*and Istituto Nazionale di Ottica Applicata, CNR, L. go E. Fermi, 6, I-50125, Florence, Italy*

(Received 7 April 2008; published 25 August 2008)

A quantum state is nonclassical if its Glauber-Sudarshan  $P$  function fails to be interpreted as a probability density. This quantity is often highly singular, so that its reconstruction is a demanding task. Here we present the experimental determination of a well-behaved  $P$  function showing negativities for a single-photon-added thermal state. This is a direct visualization of the original definition of nonclassicality. The method can be useful under conditions for which many other signatures of nonclassicality would not persist.

DOI: [10.1103/PhysRevA.78.021804](https://doi.org/10.1103/PhysRevA.78.021804)

PACS number(s): 42.50.Dv, 42.50.Xa, 03.65.Ta, 03.65.Wj

Einstein's hypothetical introduction of light quanta, the photons, was the first step toward the consideration of nonclassical properties of radiation [1]. But what does nonclassicality mean in a general sense? A radiation field is called nonclassical when its properties cannot be understood within the framework of the classical stochastic theory of electromagnetism. For other systems, nonclassicality can be defined accordingly. Here we will focus our attention on harmonic quantum systems, such as radiation fields or quantum-mechanical oscillators, for example, trapped atoms.

In this context the coherent states, first considered by Schrödinger in the form of wave packets [2], play an important role. They represent those quantum states that are most closely related to the classical behavior of an oscillator or an electromagnetic wave. For a single radiation mode, the coherent states  $|\alpha\rangle$  are defined as the right-hand eigenstates of the non-Hermitian photon annihilation operator  $\hat{a}$ ,  $\hat{a}|\alpha\rangle = \alpha|\alpha\rangle$ ; cf., e.g., [3]. A general mixed quantum state  $\hat{\rho}$ ,

$$\hat{\rho} = \int d^2\alpha P(\alpha)|\alpha\rangle\langle\alpha|, \quad (1)$$

can be characterized by the Glauber-Sudarshan  $P$  function [3,4]. In this form the quantum statistical averages of normally ordered operator functions can be written as

$$\langle:\hat{f}(\hat{a}, \hat{a}^\dagger): \rangle = \int d^2\alpha P(\alpha)f(\alpha, \alpha^*), \quad (2)$$

where the normal ordering prescription  $:\hat{f}(\hat{a}, \hat{a}^\dagger):$  means that all creation operators  $\hat{a}^\dagger$  are to be ordered to the left of all annihilation operators  $\hat{a}$ .

Formally, the resulting expressions (2) for expectation values are equivalent to classical statistical mean values. However, in general, the  $P$  function does not exhibit all the properties of a classical probability density. It can become negative or even highly singular. Within the chosen representation of the theory, the failure of the Glauber-Sudarshan  $P$

function to show the properties of a probability density is taken as the key signature of quantumness [5,6].

In this Rapid Communication we demonstrate the experimental determination of a nonclassical  $P$  function. Within the experimental precision it clearly attains negative values. This is a direct demonstration of nonclassicality: the negativity of the  $P$  function prevents its interpretation as a classical probability density.

Why is it so difficult to demonstrate the nonclassicality directly on the basis of this original definition? Let us go back to a single photon as postulated by Einstein. Its  $P$  function is

$$P(\alpha) = \left(1 + \frac{\partial}{\partial\alpha} \frac{\partial}{\partial\alpha^*}\right) \delta(\alpha); \quad (3)$$

cf., e.g., [7]. Already in this case we get a highly singular distribution in terms of derivatives of the  $\delta$  distribution, which cannot be interpreted as a classical probability. Due to these properties, it is difficult to experimentally determine nonclassical  $P$  functions in general.

How can one realize nonclassical states whose properties can be demonstrated directly in terms of the original definition, that the  $P$  function fails to be a probability density? This question is not trivial: for instance, losses introduced by imperfect experimental efficiencies lead only to rescaling of the quadrature variable; cf., e.g., [8]. The  $P$  function obtained by perfect detection is related to  $P_\eta(\alpha)$ , obtained with the quantum efficiency  $\eta$  via

$$P(\alpha) = \eta P_\eta(\sqrt{\eta}\alpha). \quad (4)$$

Consequently, singularities in the  $P$  function are then preserved. Most of the nonclassical states experimentally generated so far have highly singular  $P$  functions, whose reconstruction is impossible. However, one may start with a thermal state  $\hat{\rho}_{\text{th}}$  with mean photon number  $\bar{n}$ . By photon creation one gets a single-photon-added thermal state

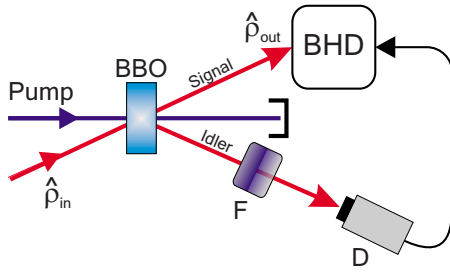


FIG. 1. (Color online) Scheme for the conditional excitation of a thermal light state (denoted by  $\hat{\rho}_{in}$ ) by a single photon. A click in the on-off detector  $D$  prepares the photon-added thermal state  $\hat{\rho}_{out}$  and triggers its balanced homodyne detection (BHD).

(SPATS),  $\hat{\rho} = \mathcal{N} \hat{a}^\dagger \hat{\rho}_{th} \hat{a}$ , where  $\mathcal{N}$  denotes the normalization. Its  $P$  function is now well behaved, but violates the properties of a classical probability density [9],

$$P(\alpha) = \frac{1}{\pi \bar{n}^3} [(1 + \bar{n})|\alpha|^2 - \bar{n}] e^{-|\alpha|^2/\bar{n}}, \quad (5)$$

giving rise to the question of whether its experimental determination could be possible [10]. In the zero-temperature limit, the SPATS includes the special case of the one-photon Fock state with the highly singular  $P$  function given in Eq. (3). In this sense the SPATS represents a single photon whose  $P$  function is regularized by a controlled thermal background.

Recently, SPATSs could be realized experimentally and some of their nonclassical signatures have been verified [11]. Nevertheless, the reconstruction of a nonclassical  $P$  function remains a challenging problem which goes beyond the standard procedures of quantum state reconstruction; for the latter, see, e.g., [7]. A successful determination of the  $P$  function of a SPATS would visualize the basic definition of nonclassicality for a quantum state that lies at the heart of Einstein's hypothesis: a regularized version of a single photon.

The core of the experimental apparatus used to produce SPATSs is an optical parametric amplifier based on a type-I  $\beta$ -barium borate (BBO) crystal pumped by radiation at 393 nm (see Fig. 1). The pump is obtained by second harmonic generation in a lithium triborate (LBO) crystal of a mode-locked Ti:sapphire laser emitting 1.5 ps pulses with a repetition rate of 82 MHz. When the parametric amplifier is not injected, spontaneous parametric down-conversion takes place, generating pairs of photons at the same wavelength as the laser source along two directions commonly called the signal and idler channels. We perform a conditional preparation of the quantum states by placing an on-off photodetector ( $D$ ) after narrow spectral-spatial filters ( $F$ ) along the idler channel [11,12].

A click of the idler detector prepares the signal state, whose quadratures are measured on a pulse-to-pulse basis using an ultrafast balanced homodyne detection scheme [13]. After verifying the phase independence of the quadrature distributions, the state is then analyzed by acquiring quadrature values with random local oscillator phases. When no fields are present at the inputs of the parametric amplifier, condi-

tioned single-photon Fock states are spontaneously generated in the signal channel [12,14]. On the other hand, we have recently shown that the injection of pure or mixed states results in the conditional production of their single-photon-added versions, always converting the initial states into nonclassical ones [11,15,16].

Here we use a pseudothermal source, obtained by inserting a rotating ground glass disk in a portion of the laser beam, for injecting the parametric amplifier and producing SPATSs. The scattered light forms a random spatial distribution of speckles whose average size is larger than the core diameter of a single-mode fiber used to collect it. When the ground glass disk rotates, light exits the fiber in a clean collimated spatial mode with random amplitude and phase fluctuations, yielding the photon distribution typical of a thermal source [17]. The product between the SPATS preparation rate and the coherence time of the injected thermal state (a few microseconds, and depending on the rotation speed of the disk) is kept much smaller than 1. This condition assures that each state is prepared by adding a single photon to a coherent state having an amplitude and phase which are completely uncorrelated with respect to those of the previous one. This experimental realization of a thermal state directly recalls its  $P$  function definition, i.e., a statistical mixture of coherent states weighted by a Gaussian distribution:  $P(\alpha) = \exp(-|\alpha|^2/\bar{n})/(\bar{n}\pi)$ .

By performing measurements on single-photon Fock states and on unconditioned thermal ones, we have estimated an overall experimental efficiency of  $0.62 \pm 0.04$ . Both the limited efficiency in the state preparation ( $\approx 0.92$ ) and in homodyne detection ( $\approx 0.67$ ) degrade the expected final state by introducing unwanted losses. This does not contaminate the obtained  $P$  function; cf. Eq. (4).

Let us now proceed with the reconstruction of the  $P$  function. Its characteristic function  $\Phi(\beta)$  is related to that of the quadrature  $\hat{x}(\varphi)$  [7],

$$\Phi(\beta) = \langle : \hat{D}(\beta) : \rangle = \langle e^{i|\beta|\hat{x}[\pi/2 - \arg(\beta)]} \rangle e^{|\beta|^2/2}, \quad (6)$$

where  $\hat{D}(\beta)$  is the displacement operator. Since the measured state is independent of phase, we may neglect the arguments of  $\beta$  and  $\hat{x}$ . The expectation value on the right-hand side represents the characteristic function of the observable quadrature. It can be estimated from the sample of  $N$  measured quadrature values  $\{x_j\}_{j=1}^N$  via (cf. [18])

$$\langle e^{i|\beta|\hat{x}} \rangle \approx \frac{1}{N} \sum_{j=1}^N e^{i|\beta|x_j}. \quad (7)$$

Inserting Eq. (7) into (6), we get an estimation  $\bar{\Phi}(\beta)$  of  $\Phi(\beta)$ . The variance of this quantity can be estimated as

$$\sigma^2\{\bar{\Phi}(\beta)\} = \frac{1}{N} [e^{|\beta|^2} - |\bar{\Phi}(\beta)|^2]. \quad (8)$$

The inverse Fourier transform of  $\Phi(\beta)$  yields the  $P$  function, which for many nonclassical states does not exist as a well-behaved function. However, the sampled characteristic function converges stochastically toward the theoretical one. In our case its Fourier transform is an analytical function.

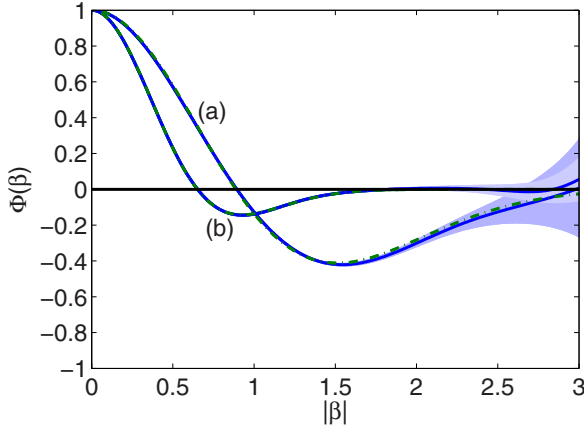


FIG. 2. (Color online) Experimental characteristic functions (solid lines) and best fit to theoretical curves (dashed lines): (a) SPATS, with  $\bar{n}=1.11$  and  $\eta=0.60$ , (b) mixture of SPATS with 19% of the thermal background, with  $\bar{n}=3.71$  and  $\eta=0.62$ . The shaded areas show the standard deviations.

For radial symmetry of the state the two-dimensional Fourier transform reduces to the Hankel transform [19],

$$P(\alpha) = \frac{2}{\pi} \int_0^{\infty} b J_0(2b|\alpha|) \Phi(b) db. \quad (9)$$

In our treatment we set the experimental curve to zero for arguments greater than a cutoff value  $|\beta|_c$ , where the graph becomes small. This limits the disturbing sampling noise on the reconstructed function

$$\bar{P}(\alpha) = \frac{2}{\pi} \int_0^{|\beta|_c} b J_0(2b|\alpha|) \bar{\Phi}(b) db \quad (10)$$

to a reasonable level. The corresponding variance has been calculated as

$$\sigma^2\{\bar{P}(\alpha)\} = \frac{1}{N} \left( \frac{4}{\pi^2} \int_0^{|\beta|_c} \int_0^{|\beta|_c} b b' J_0(2b|\alpha|) J_0(2b'|\alpha|) \bar{\Phi}(b-b') \times e^{bb'} db db' - \bar{P}(\alpha)^2 \right). \quad (11)$$

The systematic error

$$\Delta_P(\alpha) = \frac{2}{\pi} \int_{|\beta|_c}^{\infty} b J_0(2b|\alpha|) \Phi(b) db \quad (12)$$

is estimated with the help of the fitted theoretical function.

In Fig. 2 we show experimental curves for characteristic functions. Curve (a) is in good agreement with the expected characteristic function  $\Phi(\beta)$  for a SPATS,

$$\Phi(\beta) = [1 - (1 + \bar{n})|\beta|^2] e^{-\bar{n}|\beta|^2}, \quad (13)$$

for the mean thermal photon number  $\bar{n}=1.11$  and the global quantum efficiency  $\eta=0.60$ . Curve (b) shows the characteristic function for a mixture of a SPATS and its thermal background with weights of 0.81 and 0.19, respectively, for  $\bar{n}=3.71$  and  $\eta=0.62$ . For sampling these functions, we have acquired  $10^5$  and  $5 \times 10^5$  data points for the curves (a) and

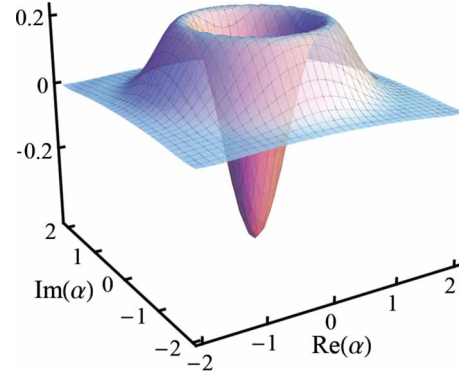


FIG. 3. (Color online) Experimentally reconstructed  $P$  function of a SPATS, as obtained from Fig. 2(a).

(b), respectively. We note that both curves are suited to reconstruct the corresponding  $P$  functions by properly choosing cutoff values  $|\beta|_c$  of their arguments.

The reconstructed  $P$  function, shown in Fig. 3, is derived from the experimental characteristic function given in Fig. 2(a). Since the measured states are independent of the phase, the reconstructed  $P$  representation is phase independent as well. It is clearly seen that the  $P$  function attains negative values, so that it fails to have the properties of a classical probability density. This is direct proof of the nonclassicality of the experimentally realized SPATS, based on the original definition of nonclassicality [5,6].

For a more careful discussion, we also examine a cross section along a radial line, as shown in Fig. 4(a). The experimentally determined curve is drawn with the solid line. Obviously, it is in good agreement with the theoretical expectation (dashed curve). The distance between the minimum value and the  $|\alpha|$  axis is approximately equal to five standard deviations, which is not diminished by the systematic error of  $|\Delta_P(\alpha)| < 0.07|P(0)|$ , obtained by the cutoff  $|\beta|_c=2.8$ . The statistically significant negativity of the  $P$  function prevents

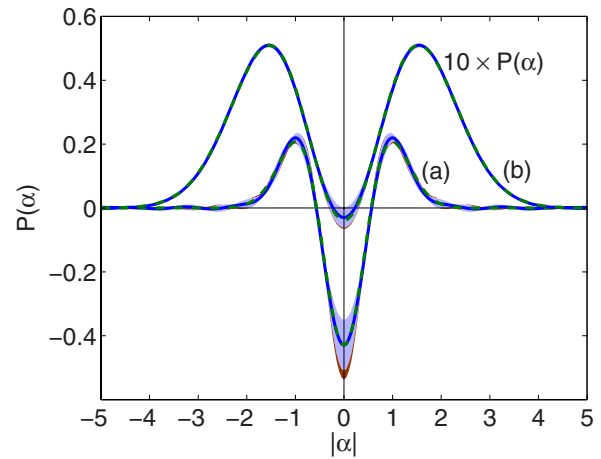


FIG. 4. (Color online)  $P$  functions (solid lines) in parts (a) and (b) are obtained from the experimental characteristic functions in Figs. 2(a) and 2(b), respectively. They are compared with the corresponding theoretical fits (dashed curves). The standard deviations (light shaded areas) and the systematic errors (dark shaded areas) are also given.

it from being interpreted as a classical probability density. This provides clear evidence of nonclassicality per definition.

Special nonclassical signatures of SPATSs, which are consequences of the negativities of the  $P$  function, have been experimentally demonstrated recently [11]. It is important to note that the reconstruction of the  $P$  function is just possible for sufficiently large thermal photon number  $\bar{n}$ . On the contrary, other criteria for nonclassicality, such as negativities of the Wigner function, the Klyshko criterion, and the entanglement potential, start to fail for increasing values of  $\bar{n}$ . To show the power of the reconstruction of the  $P$  function under such conditions, we have demonstrated its use at the limits: for a SPATS with  $\bar{n}=3.71$ , which is additionally contaminated with a 19% admixture of the corresponding thermal background. By using a cutoff  $|\beta|_c=1.9$ , we still obtain a  $P$  function being negative within one standard deviation, cf. Fig. 4(b). Other nonclassical effects, as discussed above, do not survive for this state.

Criteria for the characteristic functions are known, which are equivalent to the negativity of the  $P$  function [20]. For many states the characteristic function displays their nonclassicality by violating the condition  $|\Phi(\beta)| \leq 1$ ; cf. [21]. If the condition is satisfied,  $\Phi(\beta)$  may be integrable and then the  $P$  function can be obtained to directly verify nonclassicality. SPATSs belong to this category: for sufficiently high  $\bar{n}$  most criteria for nonclassicality (including the lowest-order one

based on the characteristic function) fail [11], but it is still possible to retrieve a negative  $P$  function.

Let us consider how sensitively the negativities of the  $P$  function depend on the overall efficiency  $\eta$ . Balanced homodyne detection measures the “true” state quadratures when the efficiency is unity. For imperfect detection ( $\eta < 1$ ) one records a convolution of the quadrature distribution with Gaussian noise, whose variance increases with decreasing  $\eta$ ; cf. [22]. In the Wigner function, this increasing noise smooths out its structures and may destroy their negativities. As can be seen from Eq. (4), the shape and the relative noise level of the reconstructed  $P$  function do not depend on the efficiency. Hence the negativities of  $P(\alpha)$  are in principle preserved even for a small efficiency, whereas for other phase-space distributions, such as the Wigner function, they are quickly lost.

In conclusion, we have reconstructed the Glauber-Sudarshan  $P$  function of an experimentally prepared single-photon-added thermal state. We obtain a well-behaved function with statistically significant negativities, so that it fails to show the properties of a classical probability density. This is a direct demonstration of nonclassicality according to its original definition. The approach works well, just when many other methods of demonstrating nonclassicality fail.

This work was partially supported by Ente Cassa di Risparmio di Firenze and CNR, under the RSTL initiative.

- 
- [1] A. Einstein, *Ann. Phys.* **17**, 132 (1905).
  - [2] E. Schrödinger, *Naturwiss.* **14**, 664 (1926).
  - [3] R. J. Glauber, *Phys. Rev.* **131**, 2766 (1963).
  - [4] E. C. G. Sudarshan, *Phys. Rev. Lett.* **10**, 277 (1963).
  - [5] U. M. Titulaer and R. J. Glauber, *Phys. Rev.* **140**, B676 (1965).
  - [6] L. Mandel, *Phys. Scr.*, T **T12**, 34 (1986).
  - [7] W. Vogel and D.-G. Welsch, *Quantum Optics*, 3rd ed. (Wiley-VCH, Weinheim, 2006).
  - [8] A. A. Semenov, D. Yu. Vasylyev, and B. I. Lev, *J. Opt. B: Quantum Semiclassical Opt.* **39**, 905 (2006).
  - [9] G. S. Agarwal and K. Tara, *Phys. Rev. A* **46**, 485 (1992).
  - [10] T. Richter, *J. Mod. Opt.* **48**, 1881 (2001).
  - [11] A. Zavatta, V. Parigi, and M. Bellini, *Phys. Rev. A* **75**, 052106 (2007).
  - [12] A. Zavatta, S. Viciani, and M. Bellini, *Phys. Rev. A* **70**, 053821 (2004).
  - [13] A. Zavatta, M. Bellini, P. L. Ramazza, F. Marin, and F. T. Arecchi, *J. Opt. Soc. Am. B* **19**, 1189 (2002).
  - [14] A. I. Lvovsky, H. Hansen, T. Aichele, O. Benson, J. Mlynek, and S. Schiller, *Phys. Rev. Lett.* **87**, 050402 (2001).
  - [15] A. Zavatta, S. Viciani, and M. Bellini, *Science* **306**, 660 (2004).
  - [16] V. Parigi, A. Zavatta, M. S. Kim, and M. Bellini, *Science* **317**, 1890 (2007).
  - [17] F. T. Arecchi, *Phys. Rev. Lett.* **15**, 912 (1965).
  - [18] A. I. Lvovsky and J. H. Shapiro, *Phys. Rev. A* **65**, 033830 (2002).
  - [19] A. J. Jerri, *Integral and Discrete Transforms with Applications and Error Analysis* (Marcel Dekker, New York, 1992).
  - [20] T. Richter and W. Vogel, *Phys. Rev. Lett.* **89**, 283601 (2002).
  - [21] W. Vogel, *Phys. Rev. Lett.* **84**, 1849 (2000).
  - [22] W. Vogel and J. Grabow, *Phys. Rev. A* **47**, 4227 (1993).